Superantigens hyperinduce inflammatory cytokines by enhancing the B7-2/CD28 costimulatory receptor interaction

Revital Levy[a,1], Ziv Rotfogel[a,1], Dalia Hillman[a], Andrey Popugailo[a], Gila Arad[a], Emmanuelle Supper[a], Farhat Osman[a], and Raymond Kaempfer[a,2]

[a]Department of Biochemistry and Molecular Biology, Institute of Medical Research Israel-Canada, The Hebrew University-Hadassah Medical School, 9112102 Jerusalem, Israel

Edited by Philippa Marrack, Howard Hughes Medical Institute, National Jewish Health, Denver, CO, and approved September 2, 2016 (received for review February 28, 2016)

Full T-cell activation requires interaction between the costimulatory receptors B7-2 and CD28. By binding CD28, bacterial superantigens elicit harmful inflammatory cytokine overexpression through an unknown mechanism. We show that, by engaging not only CD28 but also its coligand B7-2 directly, superantigens potently enhance the avidity between B7-2 and CD28, inducing thereby T-cell hyperactivation. Using the same 12-aa β-strand-hinge-α-helix domain, superantigens engage both B7-2 and CD28 at their homodimer interfaces, areas remote from where these coreceptors interact, implying that inflammatory signaling can be controlled through the receptor homodimer interfaces. Short B7-2 dimer interface mimetic peptides bind diverse superantigens, prevent superantigen binding to cell-surface B7-2 or CD28, attenuate inflammatory cytokine overexpression, and protect mice from lethal superantigen challenge. Thus, superantigens induce a cytokine storm not only by mediating the interaction between MHC-II molecule and T-cell receptor but also, critically, by promoting B7-2/CD28 coreceptor engagement, forcing the principal costimulatory axis to signal excessively. Our results reveal a role for B7-2 as obligatory receptor for superantigens. B7-2 homodimer interface mimotopes prevent superantigen lethality by blocking the superantigen–host costimulatory receptor interaction.

superantigen | cytokine storm | costimulatory receptor | B7-2 dimer interface

As principal costimulatory receptor, CD28 is a critical regulator of the immune response (1–3). Expressed constitutively on T cells, CD28 is a homodimer that interacts with its B7 coligands, transducing the signal essential for an immediate T-cell response (2–5). CD28 coligand B7-2 (CD86) is expressed constitutively on antigen-presenting cells whereas B7-1 (CD80) is induced only later (5, 6); thus, B7-2/CD28 interaction regulates early antigen signaling (7, 8).

The inflammatory cytokine response is indispensable for protective immunity, yet bacterial and viral infections often elicit an exaggerated response ("cytokine storm") harmful to the host. Thus, superantigens from *Staphylococcus aureus* and *Streptococcus pyogenes* induce toxic shock by activating an immune response, orders of magnitude beyond that elicited by regular antigens. Superantigens exploit the main axis of T-cell activation by binding directly as intact proteins to most major histocompatibility class II (MHC-II) and T-cell receptor (TCR) molecules outside their antigen-binding domains, linking them and bypassing restricted presentation of conventional antigens that typically activate <1% of T cells, thereby activating up to 20 to 30% of T cells (9–11). Moreover, T-cell activation by superantigens requires their direct binding to CD28 (12), the second signaling molecule mandatory for T-cell activation, which results in massive induction of inflammatory cytokines that mediate toxic shock, including IL-2, IFN-γ, and TNF.

Induction of human inflammatory cytokine gene expression by divergent superantigens is inhibited by a short peptide that protects mice from their lethal effect (13). The peptide shows homology to a 12-aa β-strand-hinge-α-helix superantigen domain remote from the MHC-II and TCR binding sites that, despite sequence differences among diverse superantigens, shows overall spatial conservation of the amino acid backbone (13). The family of superantigens exhibits high sequence conservation within this domain. Through this domain, essential for superantigen action (12, 13), superantigens engage CD28 directly at its homodimer interface (12). Blocking access of a superantigen to CD28, with peptide mimetics of the CD28 homodimer interface or the β-strand-hinge-α-helix superantigen domain, suffices to block signaling for overexpression of inflammatory cytokines in human peripheral blood mononuclear cells (PBMCs) and to protect mice from lethal toxic shock (12–14). The mechanism underlying the indispensable role of binding CD28 in superantigen signaling has not yet been resolved.

We show here that, through its β-strand-hinge-α-helix domain, the superantigen binds not only to the homodimer interface of CD28 but also to the homodimer interface of its coligand, B7-2. We provide a molecular mechanism for how this dual binding achieves signaling for T-cell hyperactivation. Although the two dimer interfaces (1, 15) are remote from the domains where CD28 and B7-2 engage one another, by binding both dimer interfaces, the superantigen potently enhances the interaction between B7-2 and

Significance

Superantigens—bacterial virulence factors—cause toxic shock by hyperinducing inflammatory cytokines. T-cell activation is mediated both by antigen and by interaction between principal costimulatory receptors B7-2 and CD28. Superantigens must bind CD28 to elicit cytokine overexpression through a hitherto unknown mechanism. We show that, by binding not only CD28 but also its coligand B7-2 directly, superantigens potently enhance the B7-2/CD28 interaction, thereby inducing T-cell hyperactivation. Superantigens engage B7-2 and CD28 at their homodimer interfaces, far from where the receptors interact, demonstrating the regulatory properties of these interfaces. B7-2 dimer interface peptides attenuate cytokine overexpression and prevent superantigen lethality by blocking costimulatory receptor engagement by superantigen. Thus, bacterial superantigens induce a pathogenic "cytokine storm" by strongly enhancing formation of the B7-2/CD28 costimulatory axis.

Author contributions: R.L., Z.R., G.A., F.O., and R.K. designed research; R.L., Z.R., D.H., A.P., G.A., and E.S. performed research; R.L., Z.R., and R.K. analyzed data; and R.L., Z.R., and R.K. wrote the paper.

The authors declare no conflict of interest.

This article is a PNAS Direct Submission.

[1]R.L. and Z.R. contributed equally to this work.

[2]To whom correspondence should be addressed. Email: kaempfer@hebrew.edu.

This article contains supporting information online at www.pnas.org/lookup/suppl/doi:10.1073/pnas.1603321113/-/DCSupplemental.

CD28. Thus, superantigens directly facilitate not one but two synaptic events between antigen-presenting cell and T-cell: interaction of MHC-II with TCR and interaction of B7-2 with CD28. Our findings reveal that engagement of these two costimulatory receptors can be regulated via their homodimer interfaces, a property subverted by the superantigens to their advantage.

Binding B7-2 is essential for superantigen signaling and for achieving an excessive inflammatory response. We provide a host-oriented therapeutic approach to block the indispensable interaction of the superantigen with B7-2 and CD28 dimer interfaces through short peptide mimetics of the B7-2 dimer interface. Such peptide mimetics bind diverse superantigens, prevent binding of superantigen to cell-surface B7-2 or CD28, inhibit superantigen-mediated induction of IL-2, IFN-γ, and TNF-α in human PBMCs, and are effective antagonists in vivo, protecting mice from lethal superantigen challenge.

Results

Superantigen Mimetic Peptide Inhibits Signaling Dependent on B7-2. Induction of human cytokine genes by superantigens and their lethality in mice are blocked by YNKKKATVQELD (13), a peptide variant of staphylococcal enterotoxin B (SEB) residues 150–161, TNKKKVTAQELD, the β-strand(8)/hinge/α-helix(4) domain present in divergent superantigens (13), as well as by VQYNKK-KATVQELD (p*12B*) (12). p*12B* did not inhibit induction of *IFN-γ* mRNA by αCD3, showing that it does not block signaling through the TCR (12). By contrast, this peptide severely inhibited the earlier and more pronounced induction of *IFN-γ* mRNA by αCD3 jointly with soluble B7-2, comprising its extracellular domain fused to IgG1-Fc dimer (sB7-2), a model for joint signaling through the TCR and the B7-2/CD28 costimulatory pathway (Fig. 1*A*). sB7-2 alone induced significant expression of *IFN-γ* mRNA (Fig. 1*A*) but not of IL-10 (Fig. 1*B*). sB7-2 did not augment induction of IL-10 by αCD3, and IL-10 induction by αCD3/sB7-2 was largely resistant to p*12B* (Fig. 1*B*). Thus, IL-10 induction is independent not only of CD28 (12) but also of B7-2.

Superantigens use their β-strand(8)/hinge/α-helix(4) domain to engage CD28 (12). As a mimetic of this domain, p*12B* binds directly to CD28, competing with the superantigen for its binding site and inhibiting signaling downstream from CD28 (12). The observation that p*12B* blocks B7-2–dependent *IFN-γ* induction even in the absence of SEB accordingly could be explained by a direct interaction between the peptide and CD28, resulting in attenuation of CD28 signaling. However, an alternative explanation might be that the peptide binds B7-2 and thereby inhibits signaling through the B7-2/CD28 axis. We thus considered that, through its β-strand(8)/hinge/α-helix(4) domain, the superantigen might engage B7-2 directly.

SEB Binds Cell-Surface B7-2 Directly. To examine this concept, we transfected cells to express human B7-2 having GFP fused C-terminally to its intracellular domain. SEB bound selectively to the surface of cells that expressed B7-2, with complete colocalization (Fig. 2*A*), which indicated that, even in the absence of its CD28, MHC-II, and TCR receptors, SEB binds directly to B7-2 on the cell surface. Indeed, using a second approach, immobilized sB7-2, comprising the extracellular V and C domains fused C-terminally to human IgG1 Fc, bound SEB, with binding increasing progressively with the amount of SEB (Fig. 2*B*). Using a third method, surface plasmon resonance (SPR), we detected direct binding of sB7-2 to immobilized SEB (Fig. 2*C*), but not of human IgG Fc or an unrelated control protein of the same size, ribonuclease A (Fig. S1). Binding of SEB to B7-2 (K_D, 3.4 μM) compared well with binding to CD28, which occurs with low micromolar affinity (2.3 μM) (12). A fourth method, microscale thermophoresis (MST) (16), demonstrated direct binding of SEB to B7-2 as the free proteins in solution (Fig. 2*D*) (K_D, 4.9 μM). This binding was specific: SEB did not bind the human IgG Fc control and, unlike wild-type (*wt*) SEB, *tk2* mutant $SEB^{T150A/K152A}$, carrying alanine substitutions in two highly conserved residues in the β-strand(8)/hinge/α-helix(4) domain that are critical for the binding of CD28 (12), failed to bind B7-2 (Fig. 2*D*). The *tk2* mutation severely impairs the ability of SEB to induce inflammatory cytokines in human PBMCs while abolishing its lethality, yet leaves the induction of IL-10 unabated, evidence that the ability to signal through MHC-II and TCR remains intact (12). Finally, whereas *wt* SEB bound B7-2 expressed on the cell surface, *tk2* mutant SEB failed to do so, as shown by Western blot using an anti-SEB antibody that recognizes both *tk2* and *wt* SEB (Fig. 2*E*).

SEB Uses Its β-Strand(8)/Hinge/α-Helix(4) Domain to Bind B7-2. We next immobilized β-strand(8)/hinge/α-helix(4) domain peptide p*12C* (YNKKKATVQELD abutted by Cys at both termini), which was as active as YNKKKATVQELD in blocking SEB-mediated *IFN-γ* and *IL-2* mRNA induction (12). sB7-2 bound p*12C* directly (Fig. 3*A*), and this binding was abolished by randomly scrambling the p*12C* sequence (Fig. 3*B*). Moreover, binding of B7-2 to p*12C* peptide was sensitive to pairwise alanine substitutions in residues conserved within the β-strand(8)/hinge/α-helix(4) domain (p*12YK*, p*12KD*) (Fig. 3*C*). These substitutions severely reduce binding of p*12C* to CD28 (12), demonstrating similar specificity; as mentioned above, site-directed T150A/K152A mutagenesis of SEB destroys its lethality (12). We conclude that SEB engages B7-2 directly and specifically through its β-strand(8)/hinge/α-helix(4) domain, which can explain the inhibitory effect of p*12B* on sB7-2/αCD3-mediated *IFN-γ* gene expression (Fig. 1*A*) and the loss of B7-2 binding resulting from the *tk2* mutation in SEB (Fig. 2 *D* and *E*).

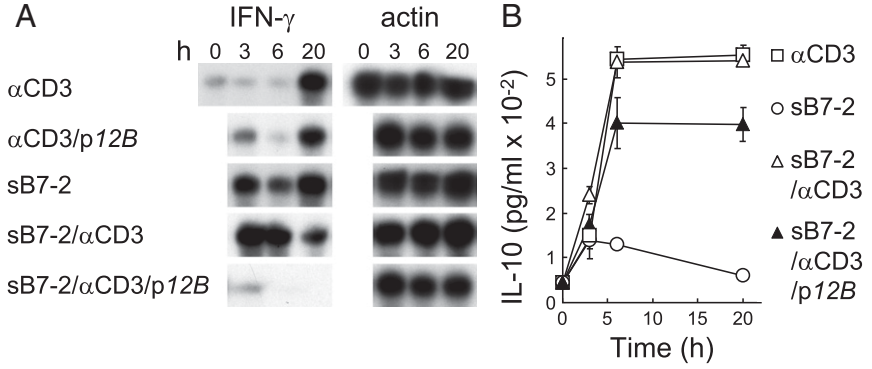

Fig. 1. Superantigen mimetic peptide blocks B7-2 signaling. (*A* and *B*) p*12B* inhibits sB7-2/αCD3-mediated induction of *IFN-γ* mRNA, but not of IL-10. Human PBMCs were incubated with αCD3 monoclonal antibody (0.1 μg/mL), sB7-2 (1 μg/mL), or both, with or without p*12B* (10 μg/mL). mRNA was quantitated by RNase protection analysis; *β-actin* mRNA indicates equal loading of RNA (*A*). Secreted IL-10 was determined (*B*).

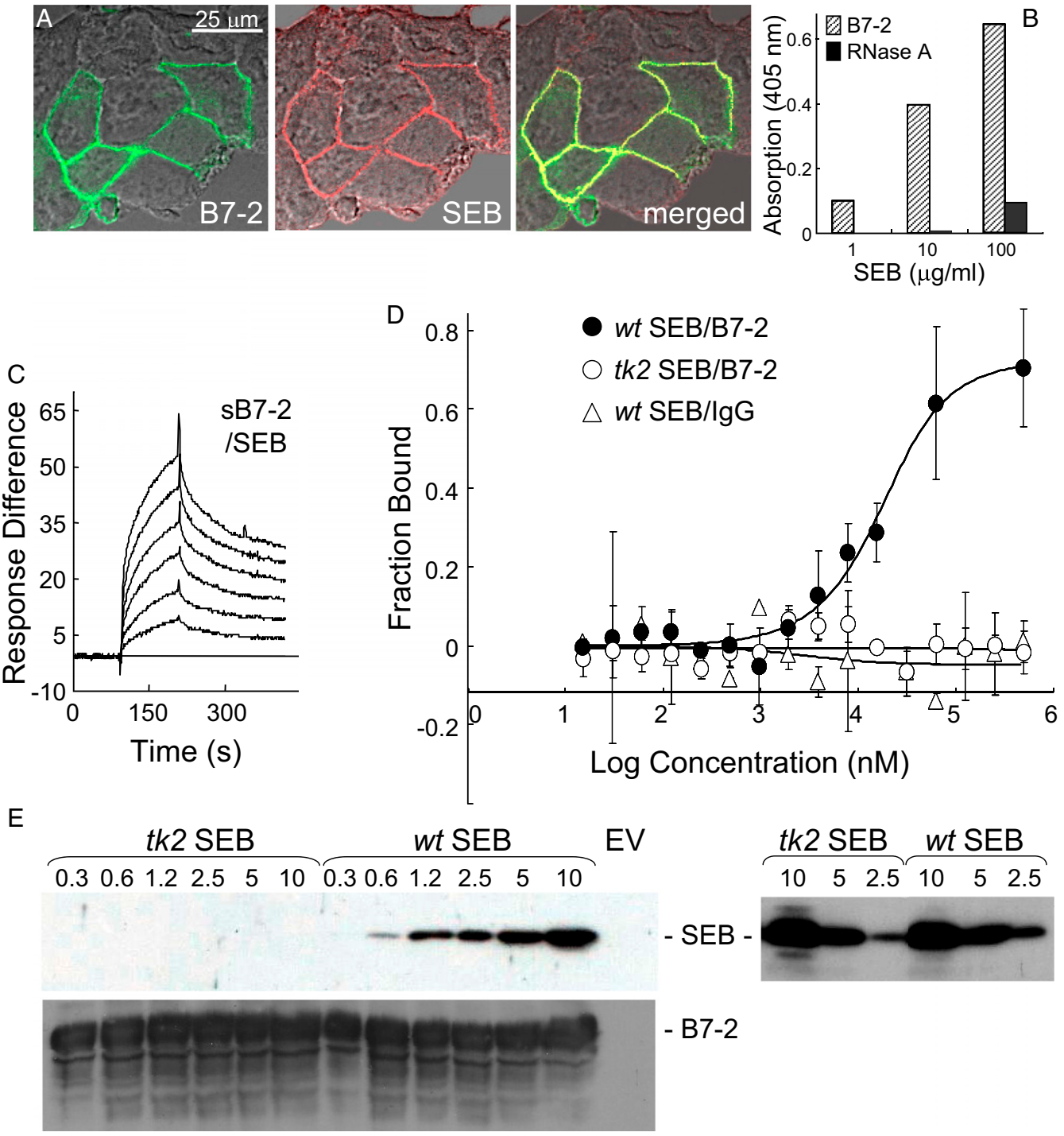

Fig. 2. Superantigen binds B7-2 directly. (*A*) Colocalization of SEB with cell-surface B7-2. Representative field of confocal microscopy is shown. HEK 293T cells were transfected to express B7-2–GFP fusion protein (green) and after 24 h incubated for 30 min with Alexa-Fluor-633–labeled SEB (red). (*B*) Binding of SEB to immobilized sB7-2 (5 μg/mL), but not to immobilized ribonuclease A (5 μg/mL), determined with anti–SEB-HRP antibody (0.2 μg/mL) in an ELISA. (*C*) Representative SPR responses for binding of B7-2-Fc in twofold increments from 0.031 μM to immobilized SEB. (*D*) SEB and B7-2 interact directly as free molecules. Representative MST responses are shown for binding of labeled *wt* or *tk2* SEB (240 nM) to increasing concentrations of B7-2-Fc or for binding of *wt* SEB to IgG Fc (error bars, SEM; $n = 3$). (*E*) Binding of SEB to cell-surface B7-2. HEK 293T cells were transfected to express B7-2 or with empty vector (EV) and after 36 h incubated for 1 h with recombinant *wt* or *tk2* mutant SEB (μg/mL). Cells were washed three times with cold PBS before lysis. Western blots of equal amounts of total cell protein (Bradford assay) with 0.1 μg/mL αSEB antibody followed by 0.2 μg/mL horseradish peroxidase-conjugated donkey anti-mouse IgG (*Top*) or with 0.1 μg/mL αB7-2 antibody followed by 0.2 μg/mL horseradish peroxidase-conjugated donkey anti-goat IgG (*Bottom*); autoradiograms are from representative experiments. On the *Right*, both *tk2* and *wt* recombinant SEB (μg/mL) were detected by Western blot with the αSEB antibody.

B7-2 Uses Its Homodimer Interface to Bind SEB. Because SEB binds into the CD28 homodimer interface (12), we investigated whether superantigens might engage B7-2 also at its dimer interface. In the B7-2/CTLA-4 complex (1), the MYPPPY domain, conserved between CD28 and CTLA-4, engages B7-2 such that the B7-2 dimer interface remains fully accessible (Fig. 4*A*). Accordingly, we

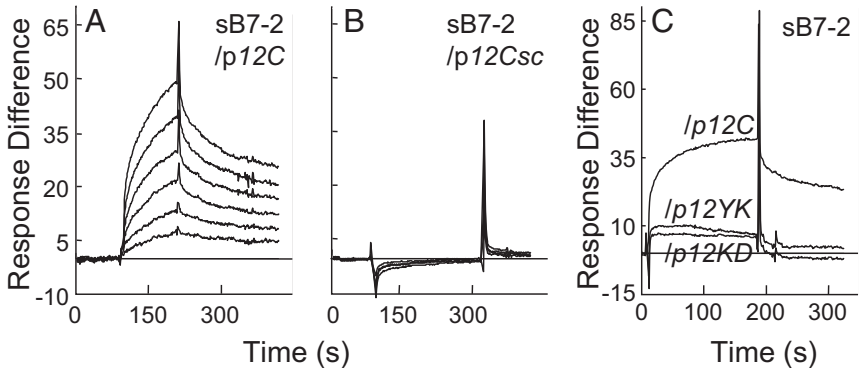

Fig. 3. SEB uses its β-strand(8)/hinge/α-helix(4) domain to bind B7-2. (*A* and *B*) Representative SPR responses for binding of B7-2-Fc in twofold increments from 0.031 μM to immobilized p*12C* (YNKKKATVQELD) (*A*) or randomly scrambled p*12Csc* (EKAKYTQLVKDN) (*B*). (*C*) Mutation of SEB β-strand(8)/hinge/α-helix(4) domain peptides reduces binding of B7-2. SPR responses to 2 μM B7-2-Fc are compared for immobilized p*12C*, p*12YK* (ANAKKATVQELD), and p*12KD* (YNAKKATVQELA) (underlined residues were mutated).

synthesized short peptides p*B2-4* and p*B2-6* overlapping residues in the B7-2 crystallographic homodimer interface (Fig. 4 *B* and *C*). As controls, we synthesized p*B2-2*, p*B2-3*, and p*B2-5*, peptides that fall outside the dimer interface (Fig. 4 *B* and *C* and Movie S1).

p*B2-2*, p*B2-3*, and p*B2-5* failed to inhibit SEB-mediated induction of IFN-γ in PBMCs whereas p*B2-4* and p*B2-6* were strongly inhibitory (Fig. 4*D*). p*B2-4* and p*B2-6*, but not the other three peptides, inhibited also induction of IL-2 and TNF-α (Fig. S2). At lower concentrations, p*B2-4* and p*B2-6* inhibited IL-2, IFN-γ, and TNF-α induction only partially, but, together, they showed pronounced synergistic inhibition (Fig. 4*E*). By contrast, IL-10 induction was resistant to p*B2-4* and p*B2-6*, alone or in combination.

Synergy between p*B2-4* and p*B2-6* might derive from the fact that they cover nonoverlapping parts of the B7-2 dimer interface (Fig. 4*B*). We next compared their activity to that of p*B2-7*, which partially overlaps p*B2-4* and p*B2-6*, covering a continuous homodimer interface domain of nine amino acids (Fig. 4 *B* and *C*). p*B2-7* inhibited SEB-mediated induction of IL-2, IFN-γ, and TNF-α to a comparable extent as p*B2-4* and p*B2-6* in combination and, like them, did not inhibit induction of IL-10 (Fig. 4*F*). Similar results were obtained with streptococcal mitogenic exotoxin Z (SMEZ), which is 40-fold more lethal than SEB (17), and with toxic shock syndrome toxin-1 (TSST-1), a superantigen having only 6% overall sequence identity with SEB yet a similar protein backbone fold in the β-strand(8)/hinge/α-helix(4) domain (13) (Fig. S3).

The ability of B7-2 dimer interface mimetic peptides to inhibit signaling for inflammatory cytokine induction by divergent superantigens suggested that these peptides compete with B7-2 in binding superantigen. Indeed, p*B2-4* and p*B2-6* each bound SEB directly, with a K_D in the micromolar range (Fig. 5 *A* and *B* and Table S1). p*B2-4* and p*B2-6* similarly bound TSST-1 and SMEZ (Fig. S4) with micromolar affinity (Table S1).

Binding of SEB to B7-2 or CD28: Reciprocal Inhibition by Dimer Interface Peptides. We next studied binding of SEB to a cell population expressing B7-2. Binding of SEB was abrogated by αB7-2 antibody but not by αCD28, a monoclonal antibody that targets a CD28 dimer interface epitope (12), showing specificity (Fig. 5*C*). Alone or in combination, B7-2 dimer interface mimetic peptides p*B2-4* and p*B2-6* effectively blocked binding of SEB to cells expressing B7-2 whereas p*B2-2*, which falls outside the dimer interface, did not inhibit (Fig. 5*C*). p*B2-7* likewise blocked binding of SEB to cells expressing B7-2, whether alone or in combination with p*B2-4* (Fig. 5*D*). The finding that B7-2 dimer interface mimetics specifically block binding of SEB to cell-surface B7-2 shows that the SEB binding site in cell-surface B7-2 is the dimer interface and strongly reinforces the results showing that these peptides bind superantigens directly and inhibit inflammatory cytokine induction.

Remarkably, p*2TA* and p*1TA*, peptides derived from the CD28 homodimer interface that bind the superantigen directly, inhibiting inflammatory cytokine induction and toxicity (12), equally inhibited binding of SEB to cells expressing B7-2 (Fig. 5 *D* and *E*). Because p*2TA* and p*1TA* bind SEB in its β-strand(8)/hinge/α-helix(4) domain (12), they compete with B7-2 for its binding site in the superantigen. In a reciprocal experiment, we transfected cells to express cell-surface CD28. Binding of SEB to such cells is abrogated by αCD28, p*1TA*, and p*2TA*, but not by αB7-2 (12). Indeed, p*B2-4*, p*B2-6*, and p*B2-7*, but not control peptide p*B2-2*, were as capable of blocking binding of SEB to cell-surface CD28 as CD28 dimer interface mimetics p*1TA* and p*2TA* (Fig. 5*F*). Thus, not only does the superantigen use its conserved β-strand(8)/hinge/α-helix (4) domain to bind to either B7-2 or CD28 at their dimer interface, but peptide mimetics of either dimer interface possess dual antagonist activity, blocking binding of superantigen to either receptor in a reciprocal manner.

B7-2 Dimer Interface Peptides Protect from SEB Lethality. We next used an accepted model for superantigen lethality, *D*-galactosamine–sensitized mice (12, 13). p*B2-4*, p*B2-6*, and p*B2-7* blocked superantigen lethality. Although only one of five control mice survived SEB challenge, four of five and five of five mice survived that received p*B2-4* and p*B2-6*, respectively, 30 min before SEB (Fig. 6*A*). Although only one of six control mice survived SEB challenge, six of six mice survived that received p*B2-7* 30 min before SEB (Fig. 6*B*). Notably, the peptides protected when present in only two- to threefold molar excess over SEB. This high efficacy supports a critical role for the B7-2 dimer interface in mediating the deleterious response to superantigens. Protection was specific: a B7-2 peptide mimetic outside the dimer interface, p*B2-2*, failed to protect mice even from a lower dose of SEB (Fig. 6*C*).

SEB Strongly Enhances the Interaction Between B7-2 and CD28. To elicit an inflammatory cytokine response, SEB must engage not only CD28 but also its coligand B7-2, raising the question how these direct interactions promote strong T-cell activation. Considering that superantigens facilitate the MHC-II/TCR interaction through direct binding (11), we hypothesized that binding of superantigen to CD28 and B7-2 might enhance their interaction. To examine this concept, we expressed CD28 or B7-2 on the cell surface and studied the effect of SEB on binding of soluble B7-2 and CD28, respectively. This strategy allowed us to measure the B7-2/CD28 interaction in the absence of multiple ligand–receptor interactions that underlie synapse formation between antigen-presenting cell and T cell, involving not only MHC-II/TCR but also numerous distinct costimulatory ligand pairs whose expression may be altered upon SEB exposure, resulting in changes in synapse strength.

SEB strongly enhanced binding of B7-2 to cell-surface CD28 (Fig. 7*A*), even at low concentrations (Fig. S5*A*). Conversely, binding of CD28 to cell-surface B7-2 was stimulated by an order of magnitude by SEB (Fig. 7*B*). Here, too, enhanced binding was detectable already at low SEB concentrations (Fig. S5*A*). SEB

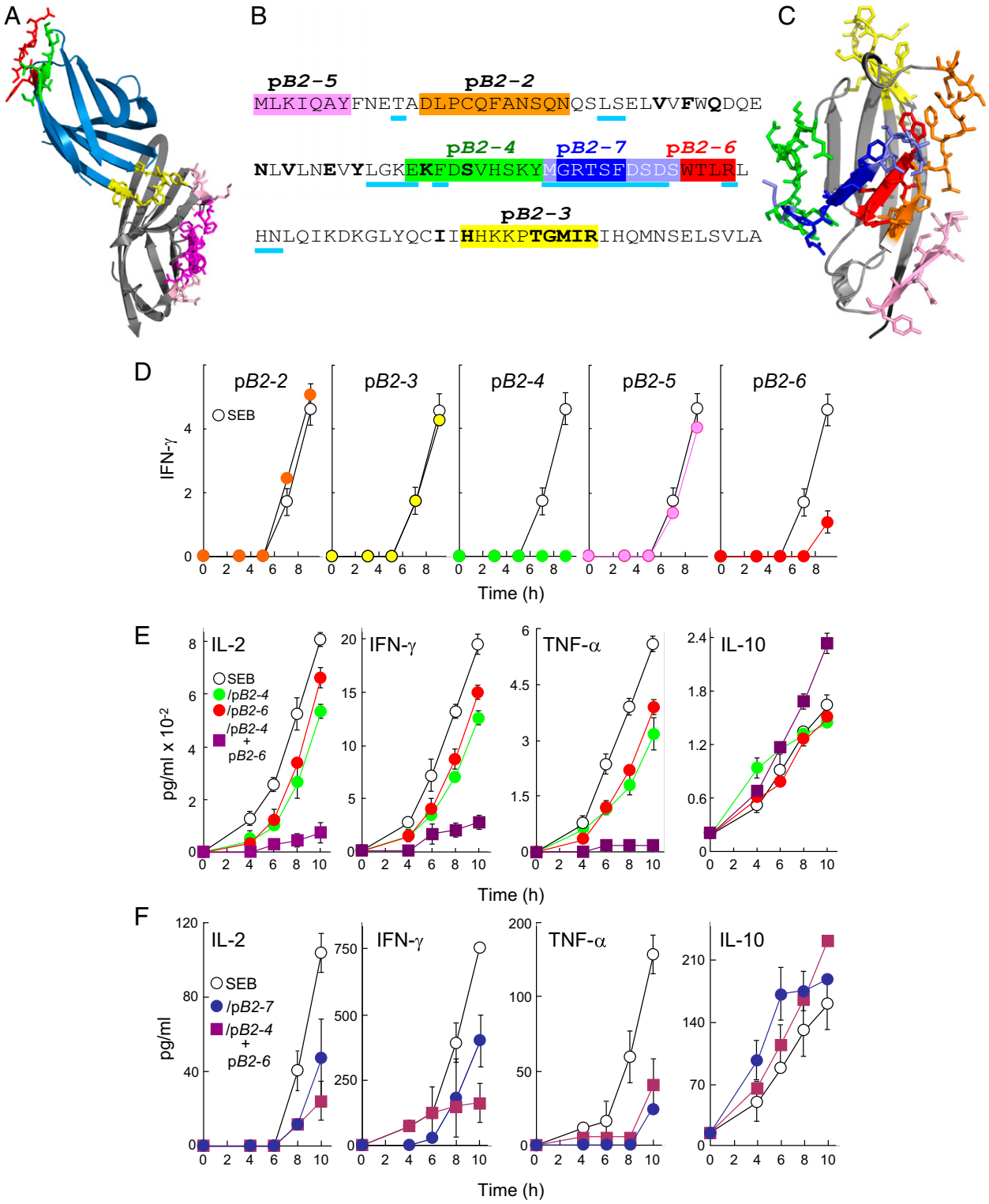

Fig. 4. Peptide mimetics of the B7-2 homodimer interface are superantigen antagonists. (*A*) In the CTLA-4/B7-2 complex (1I85.pdb) (1), B7-2 is shown in gray and CTLA-4 in blue, with homodimer interface domains of CTLA-4 in red (YVIDPE) and green (VVLASS) and its B7 binding site (MYPPPY) in yellow. Residues in the crystallographic B7-2 homodimer interface (1) are shown in magenta and pink; those in magenta are represented in mimetic peptides. (*B*) Peptide mimetics of the B7-2 dimer interface. In the extracellular domain of B7-2, residues in the dimer interface are underlined in cyan; residues that contact CTLA-4 are in boldface. Peptide sequences are marked with colors; in p*B2-7*, blue-gray residues overlap with p*B2-4* and p*B2-6*, respectively. (*C*) Location of peptides from *B* in the B7-2 structure (1I85.pdb), in corresponding colors. (*D*) Peptides p*B2-4* (EKFDSVHSKYM) and p*B2-6* (DSDSWTLR) antagonize induction of IFN-γ by SEB. PBMCs were induced with SEB (10 ng/mL), in the absence (open circles) or presence (filled circles) of 0.1 μg/mL peptide as shown. Secreted IFN-γ was determined (pg/mL $\times 10^{-2}$). (*E*) Synergy between p*B2-4* and p*B2-6*. PBMCs were induced with SEB (0.1 ng/mL), in the absence or presence of 0.01 μg/mL p*B2-4*, p*B2-6*, or both. Secreted IL-2, IFN-γ, TNF-α, and IL-10 were determined. (*F*) Superantigen antagonist activity of B7-2 dimer interface mimetic peptide p*B2-7*. PBMCs were induced with SEB (0.1 ng/mL) alone or together with 0.1 μg/mL of p*B2-7* (MGRTSFDSDS) or 0.01 μg/mL of each p*B2-4* and p*B2-6*. Secreted IL-2, IFN-γ, TNF-α, and IL-10 were determined.

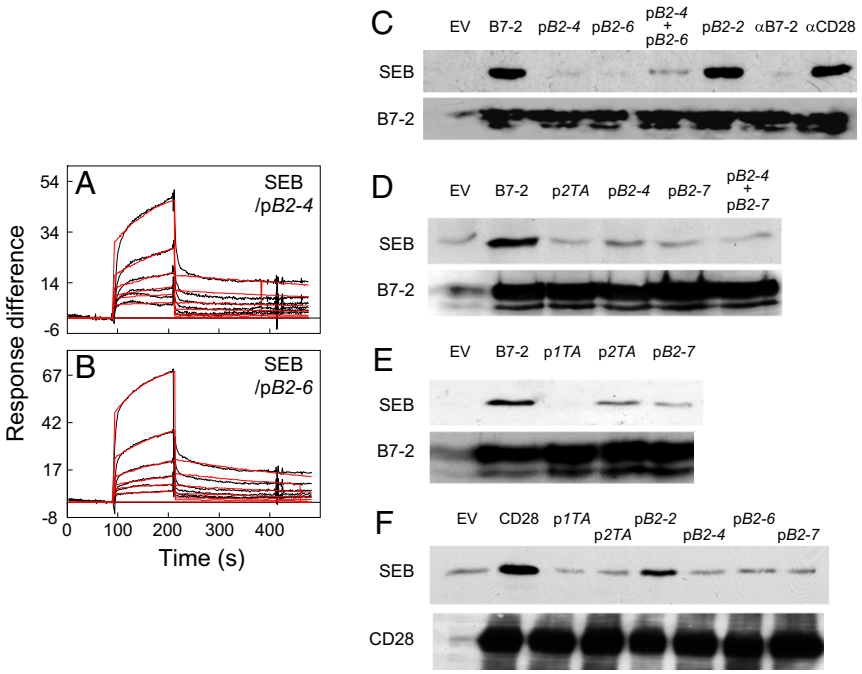

Fig. 5. Peptide mimetics of the B7-2 dimer interface bind SEB and block binding of SEB to cell-surface B7-2 and CD28. (*A* and *B*) Representative SPR responses for binding of SEB in twofold increments from 0.78 μM to immobilized p*B2-4* (*A*) and p*B2-6* (*B*); graphical fits to the binding curves are presented in red; kinetic parameters show the specificity of these interactions (Table S1). (*C–E*) Peptide mimetics of the B7-2 or CD28 homodimer interface inhibit binding of SEB to cell-surface B7-2. HEK 293T cells were transfected to express B7-2 or with empty vector (EV) and after 36 h incubated for 1 h without addition (B7-2) or as indicated, with 5 μg/mL αB7-2 antibody, αCD28 monoclonal antibody (12), or 10 μg/mL B7-2 mimetic peptides p*B2-2*, p*B2-4*, p*B2-6*, or p*B2-7*, or CD28 mimetic peptides p*1TA* or p*2TA* (12) before further incubation for 1 h with 15 μg/mL recombinant *wt* SEB. Cells were washed three times with cold PBS before lysis. Western blots of equal amounts of total cell protein with αSEB antibody (*Top*) or αB7-2 antibody (*Bottom*) were done as for Fig. 2*E*; autoradiograms are from representative experiments. (*F*) Peptide mimetics of the B7-2 or CD28 homodimer interface inhibit binding of SEB to cell-surface CD28. HEK 293T cells were transfected to express CD28 (12) or with empty vector before incubation with peptides and SEB as above. Western blots show binding of SEB to CD28 (12) (*Top*) and expression of CD28, assayed with 0.1 μg/mL αCD28 antibody (*Bottom*).

acted specifically to enhance the B7-2/CD28 interaction: Unless one of these receptors was expressed on the cell surface, SEB failed to stimulate binding of the coligand (Fig. 7 *C* and *D*).

We next used flow cytometry to validate that SEB promotes B7-2/CD28 synapse formation occurring between cells that express B7-2 and CD28, respectively, in their native state on the cell membrane (Fig. 7*E*). B7-2C, a splice variant of B7-2 unable to bind CD28 (18), failed to support significant synapse formation, demonstrating specificity. Even though flow cytometry will not distinguish a synapse formed by a single intercellular B7-2/CD28 pair from one supported by multiple pairs, rendering it less sensitive than binding of the soluble coreceptors, SEB had a pronounced stimulatory effect on B7-2/CD28-mediated intercellular synapse formation, observed already at low SEB concentrations (Fig. 7 *E–J*). Stimulation of intercellular B7-2/CD28 engagement by SEB was specific: *tk2* mutant SEB failed to do so (Fig. 7*K* and contour plots in Fig. S6).

These results provide a mechanism for why the superantigen must bind B7-2 and CD28 directly: this binding strongly upregulates the B7-2/CD28 interaction, the primary costimulatory axis mandatory for T-cell activation.

Discussion

To elicit an inflammatory cytokine storm and lethality, superantigens must bind directly to the dimer interface not only of costimulatory receptor CD28 but, as demonstrated here, also of its coligand B7-2, raising the question of how this dual binding serves the mechanism of harmful T-cell hyperactivation. Our finding is that SEB potently enhances the interaction between B7-2 and CD28. The superantigen strongly stimulates binding of B7-2 to cell-surface CD28 and vice versa (binding of CD28 to cell-surface B7-2), as well as B7-2/CD28-dependent synapse formation between cells. These results reveal a hitherto unknown function for the superantigen: to promote formation of the B7-2/CD28 costimulatory axis, critical for full T-cell activation. Thus, superantigens uniquely facilitate not one but two synaptic events between antigen-presenting cell and T cell: interaction of MHC-II with TCR, acting as intermolecular bridge (Fig. 8), and interaction of B7-2 with CD28, as revealed here, forcing the principal costimulatory axis to signal excessively. This renders the superantigen-mediated immunological synapse exceptionally strong. Our findings provide an example whereby a pathogen-associated molecule (in this case, a bacterial superantigen toxin) hyperinduces cytokines by strongly enhancing formation of the B7-2/CD28 costimulatory axis.

Our results reveal an unexpected role for B7-2 as direct superantigen receptor. Thus, superantigens make unconventional use not only of MHC-II and TCR through direct binding but also of CD28 (12) and as shown here, of B7-2. B7-2 directly senses a class of microbial virulence factors, the superantigens, broadening the scope of pathogen targets.

We used mimetic peptides as a tool to map the contact domains between superantigen and B7-2 and to show that superantigens engage B7-2 directly at its crystallographic homodimer interface. B7-2 binding is critical for superantigen action: short peptide mimetics of the B7-2 homodimer interface are potent superantigen antagonists, in vitro and in vivo. Although peptides lack the structure of the intact protein, induced fit can enable ligand binding. B7-2 dimer interface mimetic peptides compete well with cell-surface B7-2 for SEB (Fig. 5).

Our findings may be incorporated into a model in which, as for CD28 (12), the superantigen can bind simultaneously to B7-2 and MHC-II on the antigen-presenting cell and the TCR on the T cell (Fig. 8). B7-2 can be accommodated readily as a third superantigen receptor in the quaternary complex, with the B7-2 dimer interface oriented toward the β-strand(8)/hinge/α-helix(4) superantigen domain. Although this domain is buried in part, N151 and four amino acids having charged sidechains (K152, K153, K154, and E159) are exposed (Fig. 8). Considering that B7-2 and CD28 each function as a direct superantigen receptor and that the superantigen engages both through its β-strand/hinge/α-helix domain, at any given time, a single superantigen molecule can bind only one of these two costimulatory ligands. The immunological synapse contains multiple copies of each of these receptors (1). Binding of superantigen to each B7-2 and CD28 may be accommodated as shown in Fig. 8, although, conceivably, binding of the superantigen to only one receptor within a given pair, rather than to both, may suffice for T-cell

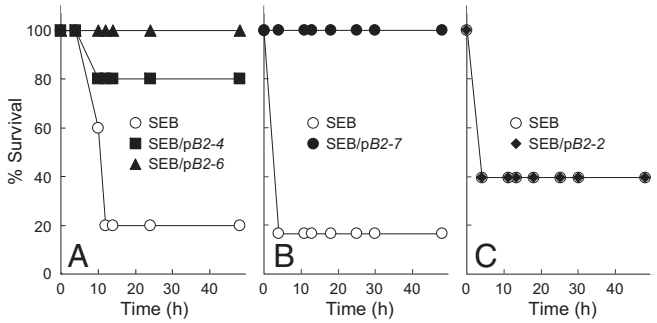

Fig. 6. Peptide mimetics of the B7-2 dimer interface protect mice from lethal SEB challenge. (*A*) Mice ($n = 5$ per group) were injected with SEB (10 μg) alone or together with 1 μg of p*B2-4* or p*B2-6*; *P* for survival, 0.022. (*B*) Mice ($n = 6$ per group) were injected with SEB (10 μg) alone or together with 0.2 μg of p*B2-7*; *P* for survival, 0.005. (*C*) Mice ($n = 10$ per group) were injected with SEB (5 μg) alone or together with 1 μg of p*B2-2*.

hyperactivation, as long as both are engaged within the immunological synapse. We have shown that the superantigen enhances the interaction between B7-2 and CD28 even without the need for engaging MHC-II and TCR (Fig. 7).

The hydrophilic B7-2 dimer interface (19) has no known role in costimulation and is well separated from the CD28 binding site (Fig. 8). Whereas CD28 is a covalent homodimer (15), B7-2 forms only an extremely weak, noncovalent homodimer and exists mostly as a monomer on the cell surface (8, 20), which renders the binding of superantigens into the B7-2 dimer interface even more remarkable. In contrast to B7-2 and CD28, SEB fails to bind the CD28 family member programmed death-1 (PD-1) (12), which lacks a functional dimer interface and is monomeric (21). Not only is the dimer interface in the extracellular domain of B7-2 well-separated from the CD28-binding site, but also, in CD28, the dimer interface is found at the opposite pole from the B7 coligand-binding site (Fig. 8). Yet, our surprising finding is that the superantigen controls B7-2/CD28 engagement through their dimer interfaces. The dependence of superantigen mechanism of action on engagement of the B7-2 and CD28 homodimer interfaces raises the possibility that these domains function also in costimulatory signaling in the absence of superantigens and that this property has been exploited by the superantigen toxins. Indeed, the avidity of CD28 for B7-2 increases after TCR signaling, and mutations in the p*1TA* dimer interface domain of CD28 (12) mimic this change, suggesting that CD28/B7-2 avidity is regulated through the CD28 dimer interface (22).

Our finding that the B7-2 homodimer interface has a direct role in transducing an inflammatory cytokine storm provided a host-oriented therapeutic approach to the sequelae of superantigen intoxication, involving blocking of the indispensable interaction of a superantigen with the B7-2 and CD28 dimer interfaces, using peptide mimetics of the B7-2 dimer interface. These peptides bind diverse superantigens, prevent binding of superantigen to cell-surface B7-2, attenuate superantigen-mediated induction of inflammatory cytokines in human PBMCs, and protect mice from lethal toxin challenge. The dimer interface of B7-2 thus serves as a therapeutic target for superantigen intoxication.

The superantigen domain that binds B7-2 is the β-strand(8)/hinge/α-helix(4) domain, remote from the MHC-II and TCR binding sites yet essential for the ability to signal into the T cell (12, 13). Despite sequence differences, the protein backbone fold of this domain shows conservation among divergent superantigens, including TSST-1 (13). Remarkably, the superantigen uses this same domain to bind CD28 directly at its homodimer interface (12). Whether mediated by SEB, SMEZ, or TSST-1, induction of IL-2, IFN-γ, and TNF-α in human PBMCs was inhibited similarly by B7-2 dimer interface mimetic peptides (Fig. 4*F* and Fig. S3), which complements the finding that CD28 dimer interface mimetic peptides inhibit inflammatory cytokine gene expression to a similar extent, whether it is induced by SEB, SEA, or TSST-1 (12). Like SEB and SMEZ, TSST-1 bound B7-2 dimer interface peptides with micromolar affinity. Indeed, peptide mimetics of either the B7-2 or CD28 dimer interface possess dual antagonist activity, interfering in a reciprocal manner with binding of superantigen to either receptor on the cell surface. This dual action, demonstrated here, may explain why p*B2-7*, a B7-2 dimer interface decapeptide mimetic, or p*2TA*, a CD28 dimer interface octapeptide mimetic (12), effectively protect mice from lethal SEB challenge, despite the fact that the 238-aa superantigen molecule interacts with MHC-II and TCR in addition to binding either B7-2 or CD28. Superantigens engage the TCR and MHC-II (23, 24) and CD28 (12), as well as B7-2, with micromolar affinity yet remain toxic even at picomolar concentrations (25). The moderate affinity of a superantigen for each of its four receptors can explain why a short mimetic peptide, binding with similarly moderate affinity, can disrupt the concerted interactions that mediate formation of the superantigen synapse and thus attenuate inflammatory cytokine hyperinduction. Although the superantigen plausibly engages a larger contact surface in its B7-2 or CD28 target, becoming stabilized at multiple sites, obstruction of a single site by a competing peptide may suffice to destroy cooperativity. Indeed, mimetic peptides from five distinct sites within the CD28 dimer interface antagonize SEB (12), and three B7-2 dimer interface mimetic peptides did so (Fig. 4).

SEB induces vigorous expression of cytokines, but only the inflammatory response, defined here by induction of IL-2, IFN-γ, and TNF-α, depends on B7-2 engagement. This need mirrors the selective requirement for CD28 signaling in induction of IL-2, IFN-γ, and TNF-α by superantigens, yet not for induction of IL-4 and IL-10 (12). By selectively attenuating IL-2, IFN-γ, and TNF-α induction, antagonist peptides will reduce the synergy between these cytokines, to allow survival. By leaving IL-10 induction intact, the peptides amplify their ability to down-regulate the inflammatory response. Conceivably, binding of superantigen to B7-2 may elicit also reverse signaling (8, 26) into antigen-presenting cells and induce inflammatory cytokines in them.

Our findings highlight the homodimer interface of the costimulatory receptors as a regulatory domain for immune signaling. We propose a twofold mechanism through which superantigens promote formation of the B7-2/CD28 axis. Binding of superantigen to B7-2 and CD28 at their homodimer interfaces, sites well removed from the domains where these costimulatory receptors interact, most plausibly induces allosteric change in each that greatly enhances their mutual affinity, thus potently stimulating their direct interaction, as we have demonstrated. Second, by directly engaging not only MHC-II and TCR but simultaneously also B7-2 or CD28, the superantigen may recruit B7-2 and CD28 into the immunological synapse. Such clustering into microdomains can enhance costimulation (27). As a result, the superantigen strongly increases signaling through the B7-2/CD28 costimulatory axis to hyperactivate inflammatory cytokine gene expression, resulting in lethality.

Experimental Procedures

Soluble B7-2 and CD28. B7-2 and CD28 expressed in mouse myeloma NS0 cells (R&D Systems) comprise the extracellular 20-239 and 19-152 amino acid domain, respectively, of the mature human ligands fused to C-terminal human IgG1 Fc and are homodimers, disulfide-linked in the Fc domain. Soluble ligands were >95% pure as judged by SDS/PAGE.

Antibodies. αSEB monoclonal antibody (clone MB2B33; Toxin Technology), horseradish peroxidase-conjugated goat anti-mouse IgG or donkey anti-goat

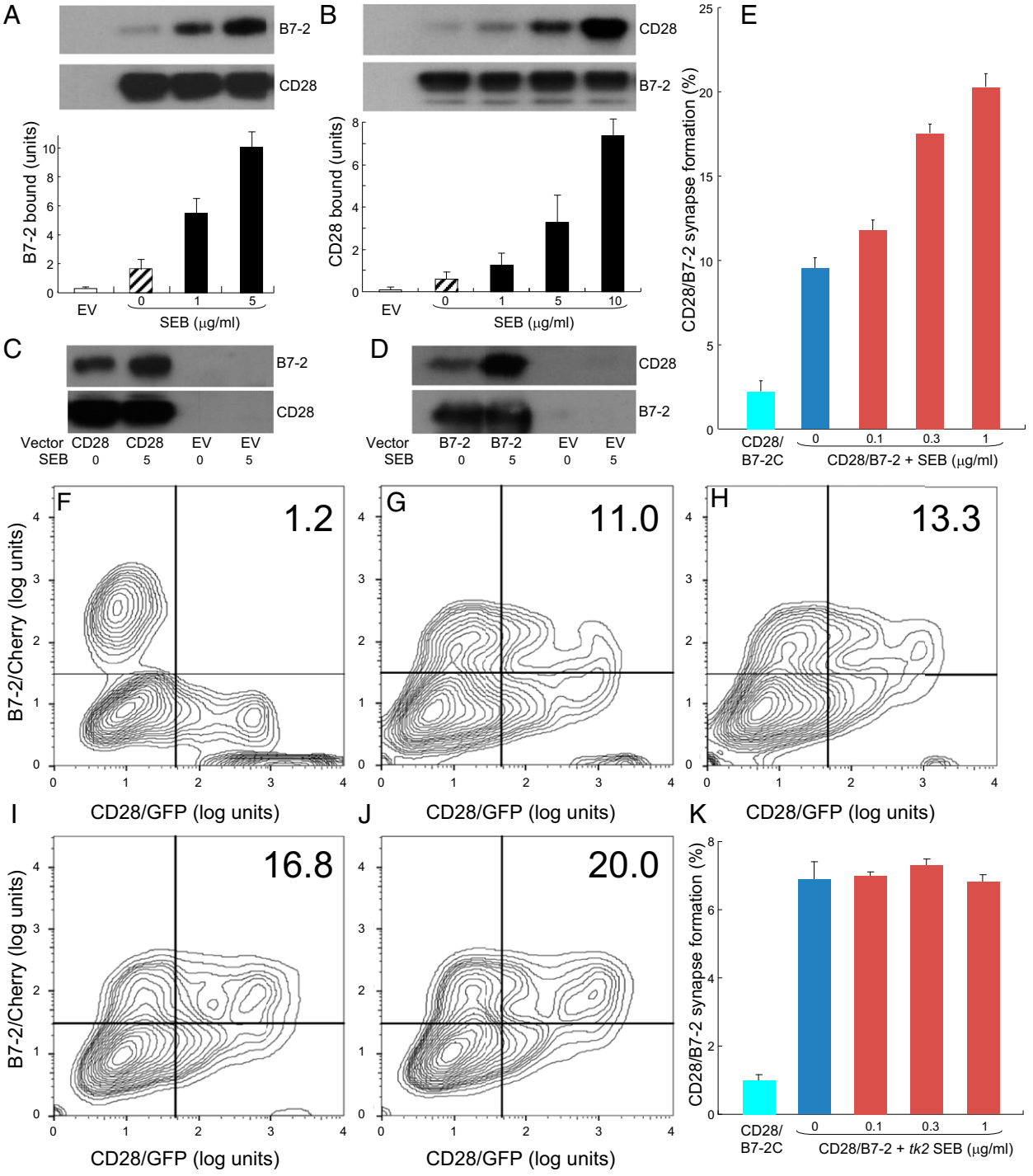

Fig. 7. The superantigen strongly enhances B7-2/CD28-dependent synapse formation. (*A*) Effect of SEB on binding of B7-2 to cell-surface CD28. HEK 293T cells were transfected to express cell-surface CD28 (12) or with empty vector (EV). Cells were incubated with soluble B7-2 in the absence or presence of SEB at concentrations shown. Western blots show binding of B7-2 and expression of CD28 by the cells. Bound B7-2 is quantitated in the bar graphs (error bars, SEM; $n = 3$). (*B*) Effect of SEB on binding of CD28 to cell-surface B7-2. HEK 293T cells were transfected to express cell-surface B7-2 or with empty vector. Cells were incubated with soluble CD28 in the absence or presence of SEB at concentrations shown. Western blots show binding of CD28 and expression of B7-2 by the cells. Bound CD28 is quantitated in the bar graphs (error bars, SEM; $n = 3$). (*C* and *D*) SEB specifically enhances the B7-2/CD28 interaction. HEK 293T cells were transfected to express cell-surface CD28 (*C*) or B7-2 (*D*) or with empty vector. Cells were incubated with soluble B7-2 (*C*) or CD28 (*D*) in the absence or presence of SEB (μg/mL). Western blots show binding of B7-2 (*C*) and CD28 (*D*) and expression of CD28 and B7-2, respectively, by the cells. Representative experiments of three are shown. (*E*) SEB enhances B7-2/CD28-mediated intercellular synapse formation. HEK 293T cells transfected to express CD28/GFP fusion protein (green label) were incubated with HEK 293T cells transfected to express B7-2/Cherry fusion protein (red label), in the absence or presence of SEB at concentrations shown. As negative control served mutant B7-2C/Cherry, which lost the ability to bind CD28. Intercellular B7-2/CD28-dependent synapse formation was scored using flow cytometry to quantitate percent doubly labeled cells (error bars, SEM; $n = 4$). (*F–J*) Contour plots are shown for a representative experiment in *E*, upon incubation of cells expressing CD28/GFP with cells expressing B7-2C/Cherry (*F*) or B7-2/Cherry (*G–J*). Incubation was done in the absence of SEB (*F* and *G*) or presence of SEB at 0.1 (*H*), 0.3 (*I*), or 1 (*J*) μg/mL. Percent doubly labeled cells in the upper right quadrant denote B7-2/CD28 synapse formation. (*K*) *tk2* mutant SEB fails to enhance B7-2/CD28-mediated intercellular synapse formation. Effect of *tk2* SEB on intercellular B7-2/CD28 engagement was analyzed by flow cytometry as in *E* (error bars, SEM; $n = 3$).

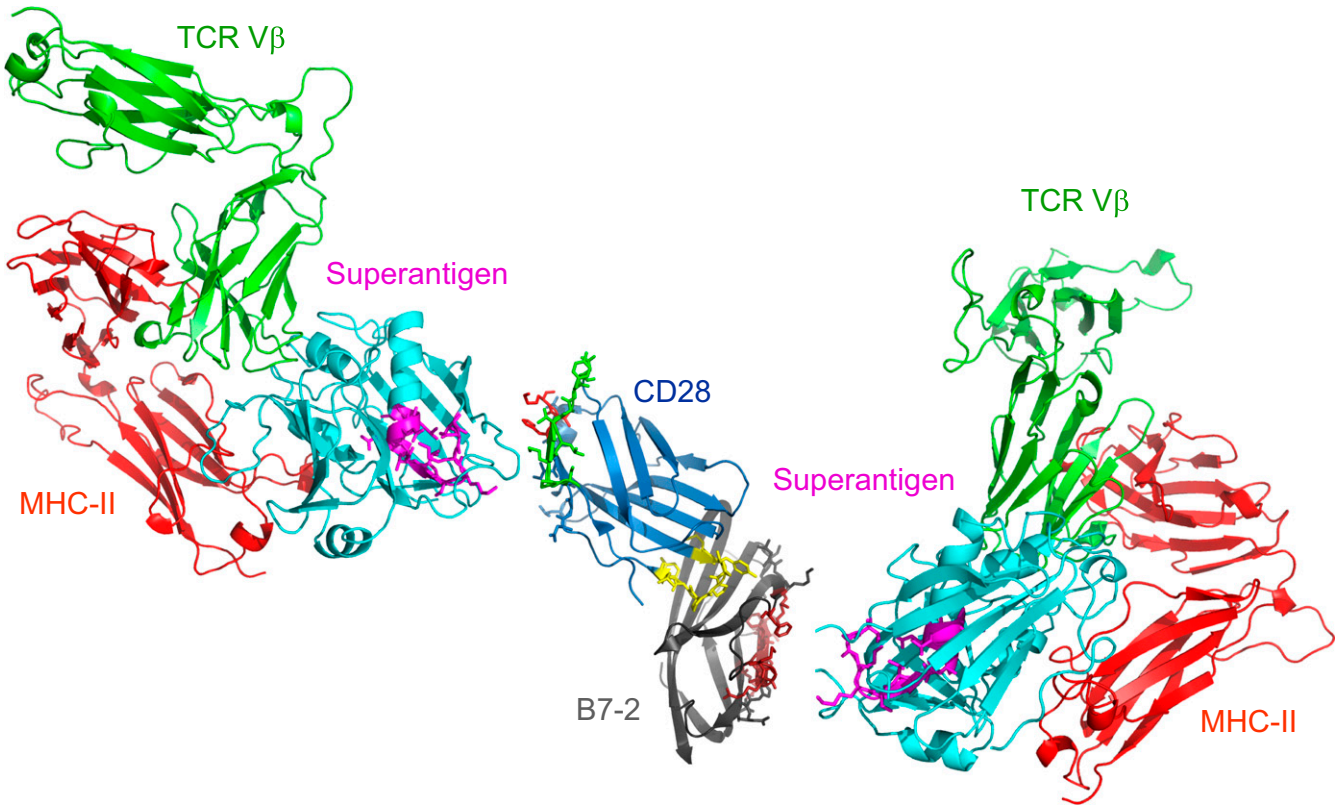

Fig. 8. Schematic model for superantigen action, requiring direct binding of superantigen to costimulatory receptors B7-2 and CD28. Two superantigen molecules (cyan) (SEC3, a close relative of SEB) in complex with TCR Vβ (green) and MHC-II (red) extracellular domains (1jck.pdb, wherein SEB/MHC-II structure is superimposed on SEC3/TCR Vβ structure) (30) engage, through their freely accessible β-strand/hinge/α-helix domain (magenta) (12), the homodimer interface of B7-2 on the right (dimer interface residues within p*B2-4*, p*B2-6*, and p*B2-7* are in brown) and the homodimer interface of CD28 on the left, respectively. Because the CD28/B7-2 complex structure remains unresolved, CD28 (1YJD.pdb) (15) was superimposed on CTLA-4 in the CTLA-4/B7-2 complex (1I85.pdb) (Fig. 4*A*); green and red CD28 dimer interface residues correspond to p*2TA* and p*1TA* (only HVK was resolved), respectively. Extracellular domains of CD28 and TCR are oriented such that they enter the T cell at the top, and those of the B7-2 and MHC-II molecule are oriented such that they enter the antigen-presenting cell at the bottom.

(KPL), mouse monoclonal αCD28 (clone 37407), αCD3 (clone UCHT1), goat polyclonal anti-CD28 and anti–B7-2 (R&D Systems) antibodies were used. Binding of SEB to immobilized B7-2-Fc and ribonuclease A was assayed in ELISAs using a corresponding horseradish peroxidase-conjugated mouse anti-SEB monoclonal antibody.

Induction of Cytokine Gene Expression. Human PBMCs were separated on Ficoll Paque (Amersham), washed twice with 50 mL of RPMI medium 1640, resuspended at 4×10^6 cells per mL and cultured in this medium supplemented with 2% (vol/vol) FCS, 2 mM glutamine, 10 mM MEM nonspecific amino acids, 100 mM Na-pyruvate, 10 mM Hepes, pH 7.2, 50 μM 2-mercaptoethanol, 100 U/mL penicillin, 100 μg/mL streptomycin, and 5 μg/mL nystatin. SEB (Lot 1430; Department of Toxinology, US Army Medical Research Institute of Infectious Diseases) (12, 13) was added to 100 ng/mL. Secreted cytokines were quantitated with Quantikine ELISA kits (R&D Systems), and are presented as means ± SEM ($n = 3$).

Ribonuclease Protection Analysis. Total RNA was extracted from aliquots of 3×10^7 PBMCs with TRIzol reagent (Invitrogen) and hybridized for 18 h at 42 °C with genomic antisense RNA probes transcribed with α-[^{32}P]UTP from DNA inserted into pBS (Promega). The 274-nt *IFN-γ* probe, a T3 transcript, is complementary to *IFN-γ* exon 3 and part of intron 3; 183 nt of this RNA are protected by *IFN-γ* mRNA (12, 13, 28). Antisense RNA probe for *β-actin* mRNA protects 245 nt.

B7-2 Expression Vectors. A vector expressing B7-2 was generated by cDNA synthesis of human CD86 (NM_175862) from total human PBMC RNA using a Verso RT-PCR kit (ABgene). CD86 cDNA was generated using KOD polymerase (Novagen) with phosphorylated PCR primers 5′-GACGTCGACGGAAGGCTTGCACAGGGT and 5′-CACGCGGCCGCCCAGGTCATGAGCCATTAAGC. The PCR product was inserted into pEGFP-N3 DNA (Clontech) that had been digested with SalII and NotI and lacked the GFP region, using a Fast-Link DNA Ligation Kit (Epicentre). Vectors expressing B7-2 fused C-terminally to GFP or Cherry were generated from a B7-2 cDNA vector template with phosphorylated PCR primers 5′-TACTCGAGATGGGACTGAGTAACATTC and 5′-GTCCGCGGTGAAGCATGTACACTTTTGTCG, deleting the *B7-2* termination codon. Upon digestion with XhoI and SacII, the PCR product was inserted either into pEGFP-N3 DNA or pmCherry-N1 DNA (Clontech). B7-2C/Cherry vector was generated from B7-2/Cherry template using primers 5′-GTCTCTCGTCCTTCCGG and 5′-CTAACTTCAGTCAACCTG.

CD28/B7-2 Interaction. To assay the effect of SEB on binding of B7-2 to CD28 on the cell, HEK 293T cells were transfected to express cell-surface CD28 (12) or with empty vector expressing GFP. After 36 h, the cells were incubated for 45 min with 0.2 μg/mL soluble B7-2 in the absence or presence of SEB. After three washes with cold PBS, cells were lysed. Equal amounts of total cell protein (Bradford assay) were subjected to 10% (wt/vol) PAGE and Western blotting to show binding of B7-2 and expression of CD28 by the cells. Conversely, the effect of SEB on binding of CD28 to B7-2 on the cell was assayed by transfecting HEK 293T cells to express cell-surface B7-2. After 36 h, the cells were incubated for 45 min with 0.2 μg/mL soluble CD28 in the absence or presence of SEB. After three washes as above, cells were lysed. Equal amounts of total cell protein were subjected to 10% (wt/vol) PAGE and Western blotting to show binding of CD28 and expression of B7-2 by the cells.

For flow cytometry, we used vectors expressing CD28/GFP (12) and B7-2/Cherry fusion proteins that leave the extracellular ligand binding domains intact. HEK 293T cells, separately transfected to express CD28/GFP (green) and B7-2/Cherry or B7-2C/Cherry (red), were coincubated for 3 h at room temperature at a concentration of 10^5 cells per mL each. Synapse formation

between cell populations was analyzed by flow cytometry (Eclipse Flow Cytometry System; Sony), scoring the percentage of events positive for green and red using FlowJo vX.0.6 software.

Recombinant Superantigens. Chromosomal DNA isolated from *S. aureus* COL, from a TSST-1–producing strain of *S. aureus*, and from a SMEZ-producing strain of *S. pyogenes* was used to clone SEB, TSST-1, and SMEZ genes, respectively, into pHTT7K (29) and express them in *E. coli* as the mature proteins with an N-terminal His_6-tag. Inserts were verified by DNA sequencing. Total protein was loaded onto a His·Bind column (Novagen) and eluted stepwise with imidazole. Recombinant proteins recovered after dialysis were >98% pure on SDS/PAGE and >98% homogeneous as monomer upon analytical gel filtration through a 1 × 30-cm Superdex 75 column calibrated with molecular weight standards (GE Healthcare-Amersham Pharmacia), from which protein was eluted at a flow rate of 1 mL/min. Recombinant SEB was lethal to mice. *tk2* mutant SEB was generated as described (12).

Surface Plasmon Resonance Spectroscopy. Proteins and peptides were diluted to 10 to 200 μg/mL in 10 mM Na acetate, pH 4.0, and immobilized on a CM5 sensorchip using an amine coupling kit and amine-thiol coupling kit (BIAcore), respectively. Analytes were injected at 20 μL/min in 25 mM Hepes, pH 7.4, 150 mM NaCl, 3.4 mM EDTA, and 0.005% surfactant P20 under conditions showing no mass transport limitation. Regeneration was with 50 mM phosphoric acid. Kinetic analyses were performed at 25 °C in a BIAcore 3000 instrument, deducting the control flow cell signal from the binding signal. Analyte curves were run in duplicate; representative results are shown. BIAevaluation 3.1 software was used to determine dissociation constant K_D in the linear ligand concentration range (1:1 Langmuir binding). Criteria for K_D determination for complexes were SE as percent of association rate k_a and dissociation rate k_d; χ^2 values well below 2 show the quality of fit between calculated and observed binding values and attest to the purity of the ligands examined. Fitting residuals were within the range of ±2, validating the goodness of fit. Human IgG (The Jackson Laboratory) and ribonuclease A (Sigma) served as controls.

Microscale Thermophoresis. SEB (20 μM) was labeled using a RED-NHS kit (NanoTemper Technologies) at 25 °C for 30 min (molar ratio dye/protein ~2.5:1). Unreacted dye was removed with dye removal columns equilibrated with PBS. Label-to-protein ratio was determined using photometry at 650 and 280 nm; typically, a ratio of 0.8 was achieved. Labeled SEB was adjusted to 480 nM with binding buffer (PBS, 0.05% Tween 20). B7-2 Fc or IgG1 Fc was dissolved in binding buffer. SEB, B7-2 Fc, and IgG1 were centrifuged for 5 min at 18,000 × *g* to remove noise-inducing aggregates. Sixteen serial 1:1 dilutions of B7-2 Fc or IgG1 were prepared in binding buffer. Each dilution was mixed with one volume of labeled SEB, yielding a final concentration of fluorescently labeled SEB of 240 nM and final Fc concentrations ranging from 15.25 nM to 500 μM. Approximately 4 μL of each solution was filled into Monolith NT Standard Treated Capillaries (NanoTemper). Thermophoresis was measured using a Monolith NT.115 instrument (NanoTemper) at 25 °C with 5 s/30 s/5 s laser off/on/off times, respectively. Instrument parameters were adjusted with 90% LED power and 40% MST power. Thermophoresis signals from three independent experiments were analyzed using NT.Analysis software version 1.5.41 (NanoTemper).

Mouse Lethality Assay. Female BALB/c mice (10 to 12 wk; Harlan) were challenged by i.p. injection of SEB and 20 mg of *D*-galactosamine to sensitize the animals to superantigens (13). Antagonist peptides were injected intraperitoneally 30 min before challenge. Survival was monitored. Viability remained constant beyond 72 h for as long as monitored (2 wk). Experiments involving mice were approved by the institutional animal care and use committee of The Hebrew University-Hadassah Medical School.

Statistical Analysis. Survival curves were analyzed using the Kaplan–Meier method, with the Log-Rank test for comparisons.

Structure Models. Schematic models of protein structure were created in PyMol (www.pymol.org).

ACKNOWLEDGMENTS. This work was supported by Grants UC1AI067231 and 2U54AI057168 from the National Institute of Allergy and Infectious Diseases.

1. Schwartz JC, Zhang X, Fedorov AA, Nathenson SG, Almo SC (2001) Structural basis for co-stimulation by the human CTLA-4/B7-2 complex. *Nature* 410(6828):604–608.
2. Sharpe AH, Freeman GJ (2002) The B7-CD28 superfamily. *Nat Rev Immunol* 2(2): 116–126.
3. Riley JL, June CH (2005) The CD28 family: A T-cell rheostat for therapeutic control of T-cell activation. *Blood* 105(1):13–21.
4. Lindsten T, et al. (1993) Characterization of CTLA-4 structure and expression on human T cells. *J Immunol* 151(7):3489–3499.
5. Collins AV, et al. (2002) The interaction properties of costimulatory molecules revisited. *Immunity* 17(2):201–210.
6. Lenschow DJ, et al. (1993) Expression and functional significance of an additional ligand for CTLA-4. *Proc Natl Acad Sci USA* 90(23):11054–11058.
7. Greenwald RJ, Freeman GJ, Sharpe AH (2005) The B7 family revisited. *Annu Rev Immunol* 23:515–548.
8. Bhatia S, Edidin M, Almo SC, Nathenson SG (2006) B7-1 and B7-2: Similar costimulatory ligands with different biochemical, oligomeric and signaling properties. *Immunol Lett* 104(1-2):70–75.
9. Marrack P, Blackman M, Kushnir E, Kappler J (1990) The toxicity of staphylococcal enterotoxin B in mice is mediated by T cells. *J Exp Med* 171(2):455–464.
10. Miethke T, et al. (1992) T cell-mediated lethal shock triggered in mice by the superantigen staphylococcal enterotoxin B: Critical role of tumor necrosis factor. *J Exp Med* 175(1):91–98.
11. Leder L, et al. (1998) A mutational analysis of the binding of staphylococcal enterotoxins B and C3 to the T cell receptor beta chain and major histocompatibility complex class II. *J Exp Med* 187(6):823–833.
12. Arad G, et al. (2011) Binding of superantigen toxins into the CD28 homodimer interface is essential for induction of cytokine genes that mediate lethal shock. *PLoS Biol* 9(9):e1001149.
13. Arad G, Levy R, Hillman D, Kaempfer R (2000) Superantigen antagonist protects against lethal shock and defines a new domain for T-cell activation. *Nat Med* 6(4): 414–421.
14. Ramachandran G, et al. (2013) A peptide antagonist of CD28 signaling attenuates toxic shock and necrotizing soft-tissue infection induced by *Streptococcus pyogenes*. *J Infect Dis* 207(12):1869–1877.
15. Evans EJ, et al. (2005) Crystal structure of a soluble CD28-Fab complex. *Nat Immunol* 6(3):271–279.
16. Wienken CJ, Baaske P, Rothbauer U, Braun D, Duhr S (2010) Protein-binding assays in biological liquids using microscale thermophoresis. *Nat Commun* 1:100.
17. Proft T, Moffatt SL, Berkahn CJ, Fraser JD (1999) Identification and characterization of novel superantigens from *Streptococcus pyogenes*. *J Exp Med* 189(1):89–102.
18. Kapsogeorgou EK, Moutsopoulos HM, Manoussakis MN (2008) A novel B7-2 (CD86) splice variant with a putative negative regulatory role. *J Immunol* 180(6):3815–3823.
19. Zhang X, Schwartz JC, Almo SC, Nathenson SG (2003) Crystal structure of the receptor-binding domain of human B7-2: Insights into organization and signaling. *Proc Natl Acad Sci USA* 100(5):2586–2591.
20. Bhatia S, Edidin M, Almo SC, Nathenson SG (2005) Different cell surface oligomeric states of B7-1 and B7-2: Implications for signaling. *Proc Natl Acad Sci USA* 102(43): 15569–15574.
21. Zhang X, et al. (2004) Structural and functional analysis of the costimulatory receptor programmed death-1. *Immunity* 20(3):337–347.
22. Sanchez-Lockhart M, et al. (2014) T cell receptor signaling can directly enhance the avidity of CD28 ligand binding. *PLoS One* 9(2):e89263.
23. Seth A, et al. (1994) Binary and ternary complexes between T-cell receptor, class II MHC and superantigen in vitro. *Nature* 369(6478):324–327.
24. Redpath S, Alam SM, Lin CM, O'Rourke AM, Gascoigne NR (1999) Cutting edge: Trimolecular interaction of TCR with MHC class II and bacterial superantigen shows a similar affinity to MHC:peptide ligands. *J Immunol* 163(1):6–10.
25. Kotb M (1995) Bacterial pyrogenic exotoxins as superantigens. *Clin Microbiol Rev* 8(3): 411–426.
26. Orabona C, et al. (2004) CD28 induces immunostimulatory signals in dendritic cells via CD80 and CD86. *Nat Immunol* 5(11):1134–1142.
27. Viola A, Schroeder S, Sakakibara Y, Lanzavecchia A (1999) T lymphocyte costimulation mediated by reorganization of membrane microdomains. *Science* 283(5402):680–682.
28. Ben-Asouli Y, Banai Y, Pel-Or Y, Shir A, Kaempfer R (2002) Human interferon-γ mRNA autoregulates its translation through a pseudoknot that activates the interferon-inducible protein kinase PKR. *Cell* 108(2):221–232.
29. Guerrier-Takada C, Eder PS, Gopalan V, Altman S (2002) Purification and characterization of Rpp25, an RNA-binding protein subunit of human ribonuclease P. *RNA* 8(3): 290–295.
30. Fields BA, et al. (1996) Crystal structure of a T-cell receptor beta-chain complexed with a superantigen. *Nature* 384(6605):188–192.

Supporting Information

Levy et al. 10.1073/pnas.1603321113

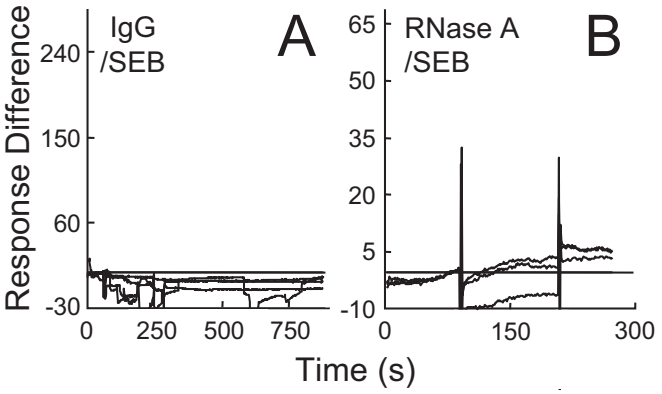

Fig. S1. Control proteins do not bind SEB. (*A* and *B*) Representative surface plasmon resonance responses for binding of IgG in four twofold increments from 0.25 μM (*A*) and for binding of 0.1, 0.3, and 1 μM ribonuclease A (*B*) to immobilized SEB, using the chip of Fig. 2*C*.

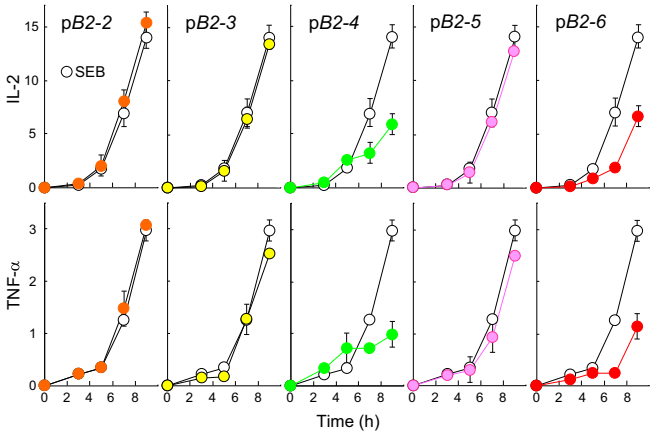

Fig. S2. Peptide mimetics of the B7-2 homodimer interface are superantigen antagonists. Peptides p*B2-4* and p*B2-6* antagonize induction of IL-2 and TNF-α by SEB. PBMCs were activated by SEB (10 ng/mL) in the absence (open circles) or presence (filled circles) of 0.1 μg/mL peptide as shown. Secreted IL-2 and TNF-α were determined. Colors correspond to those in Fig. 4*B*. Data are from the experiment shown in Fig. 4*D*.

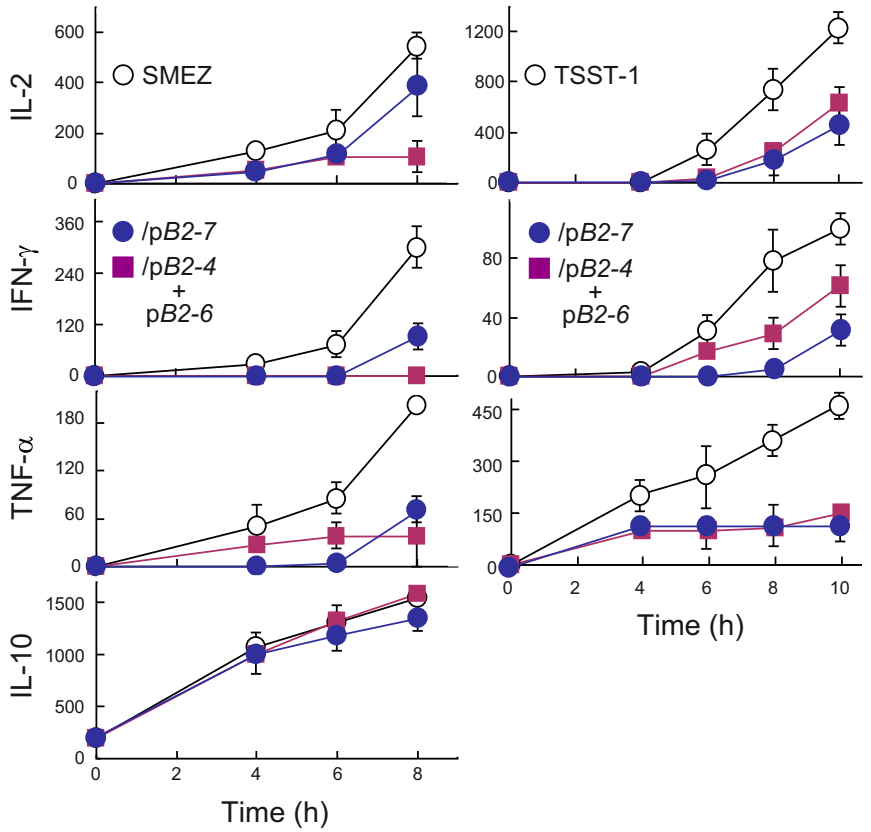

Fig. S3. Superantigen antagonist activity of B7-2 homodimer interface mimetic peptide p*B2-7*. PBMCs were incubated with 0.01 ng/mL SMEZ (*Left*) or TSST-1 (*Right*) alone or together with 0.1 μg/mL p*B2-7* or 0.01 μg/mL each p*B2-4* and p*B2-6*. Secreted cytokines were determined.

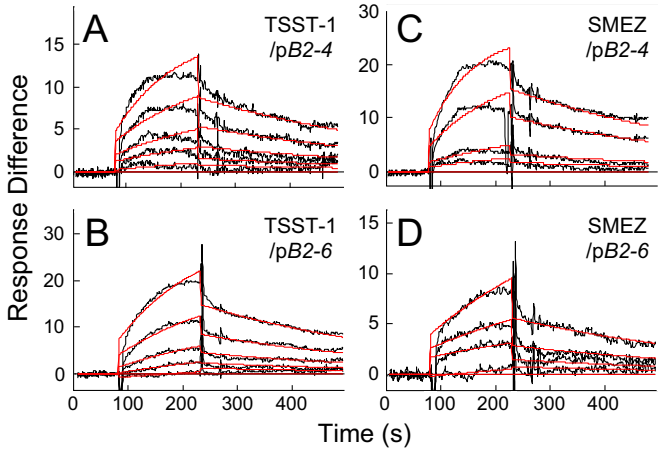

Fig. S4. B7-2 homodimer interface peptides p*B2-4* and p*B2-6* bind TSST-1 and SMEZ. (*A–D*) Representative SPR responses for binding of TSST-1 in five twofold increments from 0.0625 μM and of SMEZ in four twofold increments from 0.0625 μM to immobilized p*B2-4* or p*B2-6*, using the chips of Fig. 5 *A* and *B*. Graphical fits to the binding curves are presented in red; kinetic parameters show the specificity of these interactions (Table S1).

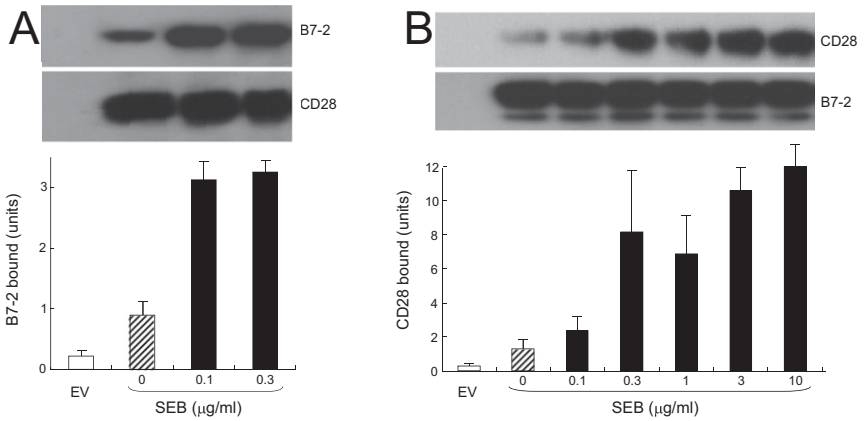

Fig. S5. SEB acts specifically to enhance the interaction between CD28 and B7-2. (*A*) Low concentrations of SEB stimulate binding of B7-2 to CD28-transfected cells. HEK 293T cells were transfected to express cell-surface CD28 or with empty vector (EV). Cells were incubated with soluble B7-2 in the absence or presence of the indicated concentrations of SEB. Western blots show binding of B7-2 and expression of CD28 by the cells. Bound B7-2 is quantitated in the bar graphs (means ± SEM; $n = 3$). (*B*) Low concentrations of SEB stimulate binding of CD28 to B7-2–transfected cells. HEK 293T cells were transfected to express cell-surface B7-2 or with empty vector. Cells were incubated with soluble CD28 in the absence or presence of the indicated concentrations of SEB. Western blots show binding of CD28 and expression of B7-2 by the cells. Bound CD28 is quantitated in the bar graphs (means ± SEM; $n = 3$).

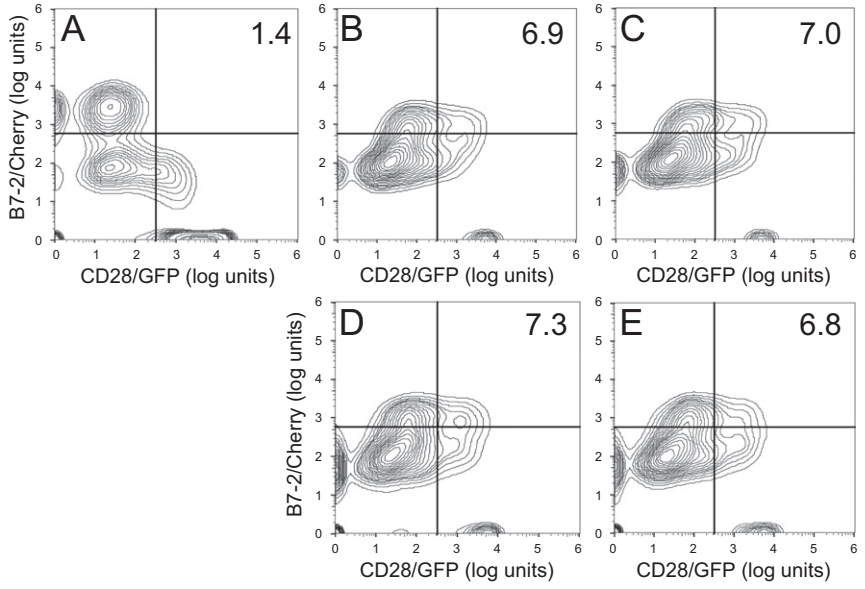

Fig. S6. *tk2* mutant SEB fails to enhance the interaction between CD28 and B7-2. (*A–E*) Contour plots are shown for a representative experiment in Fig. 7*K*, upon incubation of cells expressing CD28/GFP with cells expressing B7-2C/Cherry (*A*) or B7-2/Cherry (*B–E*). Incubation was done in the absence of *tk2* SEB (*A* and *B*) or presence of *tk2* SEB at 0.1 (*C*), 0.3 (*D*), or 1 (*E*) μg/mL. Percent doubly labeled cells in the upper right quadrant denote B7-2/CD28 synapse formation.

Table S1. Kinetic parameters of surface plasmon resonance analysis with B7-2 mimetic peptides

Fig.	Ligand	Analyte	k_a, 1/ms	SEM, k_a	% SEM, k_a/k_a	k_d, 1/s	SEM, k_d	% SEM, k_d/k_d	K_D, μM	χ^2
5*A*	p*B2-4*	SEB	413	10.30	2.50	9.58E−04	4.59E−05	4.80	2.32	1.05
5*B*	p*B2-6*	SEB	491	8.79	1.80	1.9E−03	3.69E−05	1.94	3.90	1.07
S4*A*	p*B2-4*	TSST-1	4,080	159.00	3.90	2.77E−03	8.00E−05	2.89	9.80	0.24
S4*B*	p*B2-6*	TSST-1	2,530	95.40	3.77	3.04E−03	5.92E−05	1.95	1.20	0.20
S4*C*	p*B2-4*	SMEZ	3,020	85.00	2.81	2.93E−03	9.32E−05	3.18	7.30	0.40
S4*D*	p*B2-6*	SMEZ	1,590	50.60	3.18	2.86E−03	1.34E−04	4.69	1.79	0.12

Purified recombinant superantigens were used. Concentrations of SEB ranged from 0.78 μM in six twofold increments; concentrations of TSST-1 ranged from 0.0625 μM in five twofold increments; and concentrations of SMEZ ranged from 0.0625 μM in four twofold increments. k_a, association rate; k_d, dissociation rate. BIAevaluation 3.1 software (BIAcore) was used to determine K_D in the linear ligand concentration range (1:1 Langmuir binding). Criteria for K_D determination for complexes were SE as percent of k_a and k_d; χ^2 values well below 2 show the quality of fit between calculated and observed binding values and attest to the purity of the ligands examined. Fitting residuals were within the range of ±2, validating the goodness of fit.

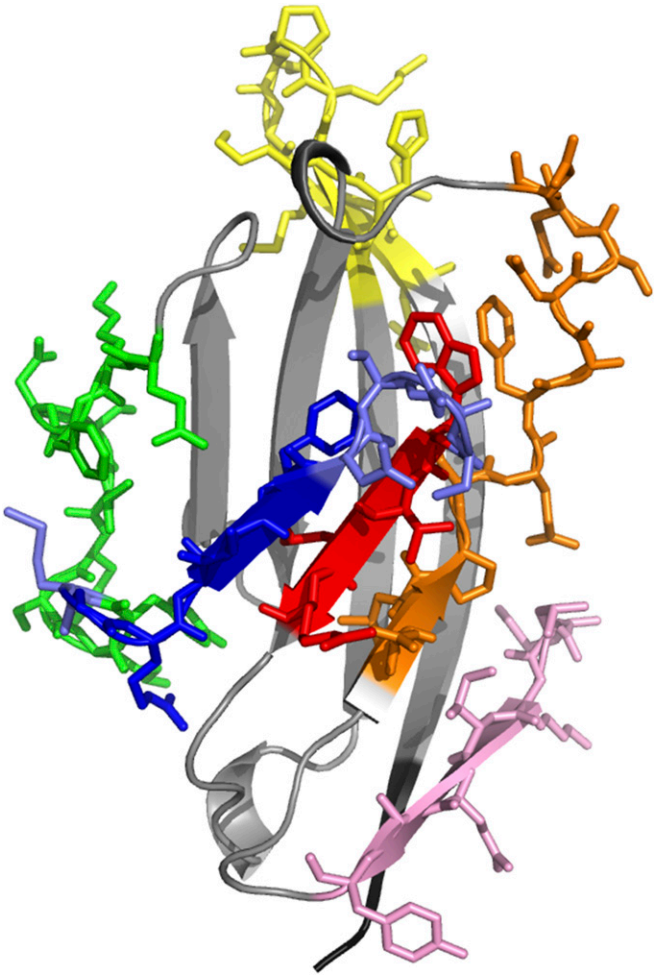

Movie S1. Location of mimetic peptides in the folded B7-2 monomer. Colors correspond to those in Fig. 4*B*. In the B7-2 extracellular domain (1I85.pdb), blue-gray residues overlap between homodimer interface peptides p*B2-4* (green) and p*B2-7* (dark blue) and between p*B2-7* and p*B2-6* (red), respectively. Peptides outside the homodimer interface are p*B2-2* (orange), p*B2-3* (yellow), and p*B2-5* (pink).

Movie S1